

## **Modeling intermittent wavepackets and their radiated sound in a turbulent jet**

By P. Jordan<sup>†</sup>, T. Colonius<sup>‡</sup>, G. A. Brès<sup>¶</sup>,  
M. Zhang<sup>†</sup>, A. Towne<sup>‡</sup> AND S. K. Lele

We use data from a new, carefully validated, Large Eddy Simulation (LES) to investigate and model subsonic, turbulent, jet noise. Motivated by the observation that sound-source dynamics are dominated by instability waves (wavepackets), we examine mechanisms by which their intermittency can amplify their noise radiation. Two scenarios, both involving wavepacket evolution on time-dependent base flows, are investigated. In the first, we consider that the main effect of the changing base flow consists in different wavepacket ensembles seeing different steady mean fields, and having, accordingly, different acoustic efficiencies. In the second, the details of the base-flow time dependence also play a role in wavepacket sound production. Both short-time-averaged and slowly varying base flows are extracted from the LES data and used in conjunction with linearized wavepacket models, namely, the Parabolized Stability Equations (PSE), the One-Way Euler Equations (OWE), and the Linearized Euler Equations (LEE). All results support the hypothesized mechanism: wavepackets on time-varying base flows produce sound radiation that is enhanced by as much as 20dB in comparison to their long-time-averaged counterparts, and ensembles of wavepackets based on short-time-averaged base flows display similar amplification. This is not, however, sufficient to explain the sound levels observed in the LES and experiments. Further work is therefore necessary to incorporate two additional factors in the linear models, body forcing by turbulence and realistic inflow forcing, both of which have been identified as potentially important in producing the observed radiation efficiency.

---

### **1. Introduction**

The recent availability of rich data from simulation and experiment for high Reynolds-number, high-speed jets has motivated new approaches to answer old questions: how is the radiated sound field related to the turbulence structure, and how might the turbulence be tamed to reduce it? Data analysis and modeling to date support a wavepacket theory of jet noise that might answer these questions (Jordan & Colonius 2013). Wavepackets are structures in jets that are correlated over large distances (many jet diameters), and whose wavelength, amplitude, and phase speed vary slowly over these distances. Unless the jet is strongly forced these structures are not particularly energetic, comprising only a small fraction of the turbulence kinetic energy. Their large spatial coherence, on distances comparable to an acoustic wavelength, and spatial growth-and-decay cycle, are two features that account for their importance as a source of sound.

The spatial structure (axial envelope, cross-stream, and azimuthal variations) and phase speeds of wavepackets deduced from experiments and simulation data closely match

<sup>†</sup> Institut PPRIME, CNRS, France.

<sup>‡</sup> California Institute of Technology

<sup>¶</sup> Cascade Technologies Inc.

those of modal solutions of the governing equations linearized about the turbulent mean flow field (Gudmundsson & Colonius 2011; Cavalieri *et al.* 2013). This similarity motivates the search for reduced-order jet-noise models, but there remain unanswered questions that must be addressed if reliable models are to be constructed.

While the near field of wavepackets computed using linear theory—where the long-time average is used as base flow—exhibits compelling agreement with experiment, the associated sound field can have errors of many orders of magnitude. We hypothesize that this error is due to the absence of intermittency effects in these average wavepackets. Such intermittency, which is observed in experiments (Juvé *et al.* 1980; Koenig *et al.* 2012), results in sound amplification beyond that produced by the average wavepacket (Cavalieri *et al.* 2011; Kerhervé *et al.* 2012; Zhang *et al.* 2014). The amplification mechanism is related to the high sensitivity of the acoustic radiation to the wavepacket envelope: flow events that lead to small near-field changes in the wavepacket, can give rise to large changes in the acoustic field. Statistically speaking, the average far-field intensity depends not on the average wavepacket, but on the strongest ones that exist intermittently.

The intermittency of wavepackets can be understood in a number of ways. Mechanisms considered here involve the evolution of wavepackets on unsteady base flows, which can be thought about in two ways. On one hand, we can consider that, as wavepacket timescales are fast compared to those of the base-flow changes, different wavepacket ensembles see different steady base flows, corresponding, for instance, to short-time averages (this will be referred to as hypothesis H1 henceforth). Another point of view (hypothesis H2 hereafter) consists in considering that there is some dynamic coupling between wavepackets and the slowly changing base flow (non-linearity is here implicit).

In order to explore these hypotheses we use data from an LES that has been validated by an accompanying experiment. The computation and validation is presented in a separate report (Brès *et al.* 2014). The LES nozzle boundary layer characteristics are in close agreement with the experimentally measured ones, and the sound field is, consequently, within 0.5dB of the measurements. Hypothesis H1 is investigated by extracting an ensemble of short-time-averages from the LES and using these in conjunction with PSE and OWE. H2 is addresseed by low-pass filtering the LES data to obtain a slowly varying base flow that is used in conjunction with the LEE.

The report is organized as follows. In Section 2 details of the linear models are provided. This is followed, in Section 3, by a presentation and discussion of the results. Concluding remarks are given in Section 4.

## 2. Linear modeling

The three modeling techniques used to compute wavepackets on steady and unsteady base flows are briefly described in what follows.

### 2.1. Parabolized stability equations

The parabolized stability equations (PSE) (Herbert 1997) are an ad hoc generalization of classical linear stability theory (LST). After linearization about some steady base flow, the fluctuation is assumed to take the form:

$$\mathbf{q}'(x, r, \theta, t) = \sum_n \sum_m \hat{\mathbf{q}}_{nm}(x, r) e^{i \int_0^x \alpha_{nm}(\zeta) d\zeta} e^{im\theta} e^{-i\omega_n t}. \quad (2.1)$$

Unlike LST, both the shape function  $\hat{\mathbf{q}}_{nm}$  and wavenumber  $\alpha_{nm}$  are allowed to vary in  $x$ . After substitution of this form into the Euler equations, the shape-function can be

rapidly calculated by solving the resulting equations as a spatial initial-value-problem in which initial fluctuations are specified at the inlet and propagated downstream. The wavenumber is determined iteratively at each step in the march to minimize the  $x$  variation of the shape-function. PSE has been used previously to model near-field average wavepackets in both subsonic and supersonic jets. In particular, Gudmundsson & Colonius (2011) applied PSE to experimental data taken from a number of subsonic jets, including a Mach 0.9 jet similar to the one studied here. They found good agreement between PSE and the first POD mode of the experimental data in the near pressure field.

To achieve a stable march in PSE, elliptic effects caused by upstream propagating acoustic modes within the Euler equations must be artificially damped, either by using dissipative numerical schemes or by the explicit addition of damping terms. Because of this damping, PSE can accurately track only a single mode of the Euler equations, usually the Kelvin-Helmholtz mode, and sound radiation is consequently missing from subsonically convecting wavepackets. These shortcomings have encouraged a second approach, the one-way Euler equations, discussed in the next section.

### 2.2. One-way Euler equations

Motivated by the efficiency of PSE, Towne & Colonius (2013, 2014) recently developed a new spatial marching method called the one-way Euler equations (OWE). Using ideas originally developed for generating non-reflecting boundary conditions (Hagstrom & Warburton 2004), the linearized Euler equations are modified such that all upstream propagating modes are removed from the operator. The resulting equations are well posed as a spatial initial-value-problem, and can be stably and efficiently solved in the frequency domain by spatial marching without the need for artificial damping. As a result, the one-way Euler equations properly capture all downstream solutions, and they are capable of directly resolving the acoustic emission of wavepackets at a small fraction of the cost of direct solutions of the full linearized Euler equations (LEE).

Here, we use the LES mean flow to verify that the one-way Euler equations produce results equivalent to those obtained using LEE and to demonstrate the improvement achieved over PSE. Using each of the three methods, we compute the perturbation to the long-time-mean at  $m = 0$ ,  $St = 0.3472$  with an inlet boundary condition based on parallel linear stability theory. The resulting pressure fields are shown in Figure 1. Both PSE and OWE produce near-field wavepackets that match well with the LEE solution. However, because OWE allows for more complicated, multi-modal behavior, the OWE solution also captures the associated acoustic radiation. Overall, the LEE and OWE solutions are nearly indistinguishable, both including the radiated sound associated with the wavepacket.

### 2.3. Linearized Euler equations

The linearized Euler equations are here solved using the high-order Dispersion Relation Preserving (DRP) scheme to compute spatial derivatives and Low Dissipation and Dispersion Runge Kutta (LDDRK) for the time advancement. Non-reflecting boundary conditions are implemented using zonal characteristic filters (as per Sandberg & Sandham (2006)) and the polar singularity is treated by the use of staggered grids around  $r = 0$ .

The grid dimensions are  $n_x \times n_r = 700 \times 500$  for a computational domain  $(L_x, L_r) = (45D, 20D)$ . The grid is equispaced in the streamwise direction, while in radial direction grid points are clustered around the centerline. The scaling factor in the characteristic filter zone (CFZ) takes a half-cosine shape: at the grid boundary, the incoming character-

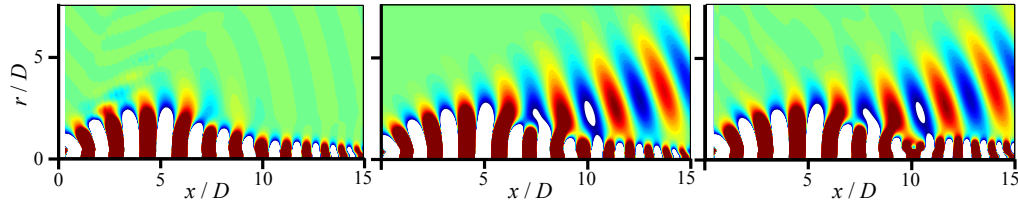


FIGURE 1. Pressure fluctuation contours for the long-time-mean base flow, forced by LST eigenfunctions. From left to right: PSE, OWE, LEE. The OWE method properly reproduces the LEE result, but at a fraction of the cost, while PSE only captures the near-field wavepacket and not its acoustic radiation. Arbitrary linear scale: the PSE and LEE are scaled to match the near-field amplitude of LES, and contours levels are chosen to highlight the acoustic radiation.

istic waves traveling into the computational domain are scaled by a factor of 0, and this factor grows smoothly to 1 where the CFZ meets the physical domain. In the streamwise direction, the length of the upstream CFZ is  $10D$  and that of the downstream CFZ is  $5D$ , where  $D$  is the exit diameter of the nozzle used in the accompanying experiments. In the radial direction, the length of outer CFZ is  $5D$ .

The unsteady base flow is obtained by low-pass filtering the LES fields at  $\text{St}_{lp} = 0.08$ . As the LES is downsampled at  $\text{St} = fD/U_j = 5.55$  (where  $f$  and  $U_j$  are, respectively, frequency and jet exit velocity) for storage, a linear interpolation is applied in order to obtain an unsteady base flow with time resolution matching that of the LEE time advancement. For comparison, LEE was also performed for the long-time-average base flow. In what follows, we refer to these different cases as ULEE and SLEE, for the unsteady and steady base-flow cases, respectively.

### 3. Results and discussion

The results are assessed by comparing the modeled hydrodynamic and acoustic fields with those of the LES. Because of the linearity of the models, it is necessary to calibrate their absolute levels for each frequency considered. This is done by means of a best match between the modeled and simulated (LES) fluctuation energy on the jet centerline, as shown in Figure 2, for instance. In what follows, we illustrate the results and conclusions by using the axisymmetric ( $m = 0$ ) mode only; similar results have been obtained for  $m = 1$  and will be documented in future papers.

As illustrated by Figure 1, for the long-time-averaged base flow, the average wavepackets predicted by PSE, OWE, and LEE agree closely with one another. Figure 2 shows that the wavepacket envelopes (in this case from LEE) are in close agreement with the full LES fluctuations over the range  $1 < x/D < 5$  (agreement extends to all Strouhal numbers considered). In the near-nozzle region,  $x/D < 1$ , previous experimental data (Cavalieri *et al.* 2013; Breakey *et al.* 2013) have shown a close match with linear models; additional work is underway to investigate the poor agreement observed with the LES data in this region. This includes analysis of the centerline data and post-processing of LES data obtained using the more refined grids described in Brès *et al.* (2014). The disagreement downstream of the end of the potential core is typical of what has been observed previously (Cavalieri *et al.* (2013); Breakey *et al.* (2013)) and is attributable to turbulence at the same frequency that is largely uncorrelated with the wavepackets. This is confirmed by the close match between the near-field wavepacket as deduced from POD of

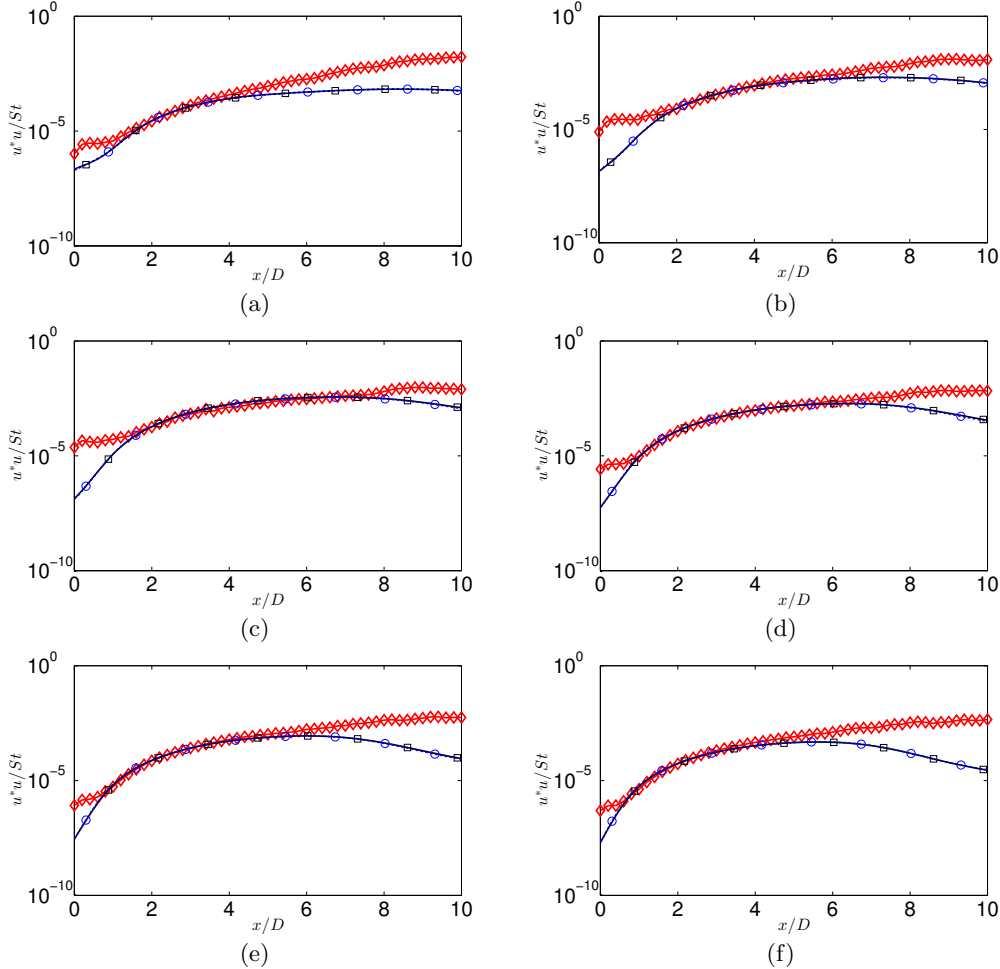


FIGURE 2. Fluctuation energy, as a function of axial position, at  $r/D = 0$ , of the streamwise velocity component for  $m = 0$  wavepackets. (a)  $St = 0.26$ . (b)  $St = 0.35$ . (c)  $St = 0.43$ . (d)  $St = 0.52$ . (e)  $St = 0.61$ . (f)  $St = 0.69$ . Solid line with diamonds: LES; solid line with squares SLEE; solid line with circles ULEE.

the LES fluctuations and the average wavepacket based on PSE of the long-time-averaged mean flow field (Figure 3).

Figure 2 shows that inclusion of the unsteady base flow does not have a large influence on the average wavepacket envelope. This is in contrast to what is observed in the acoustic field. The sound fields modeled by SLEE and ULEE are compared with the LES data on a cylindrical surface of radius  $r/D = 14.3$ . Nine axial positions on the surface are considered, corresponding to polar angles ranging from  $20^\circ$  to  $90^\circ$ . The results are shown in Figure 4. A first observation that can be made concerns the multi-lobed character of the radiation from wavepackets on the long-time-averaged base flow. This behavior, which contrasts with that observed at lower Mach number, is due to more complex interference that results from the higher degree of acoustic non-compactness of the higher-Mach-number wavepackets.

The sound radiation from the intermittent wavepackets is, as expected, less marked

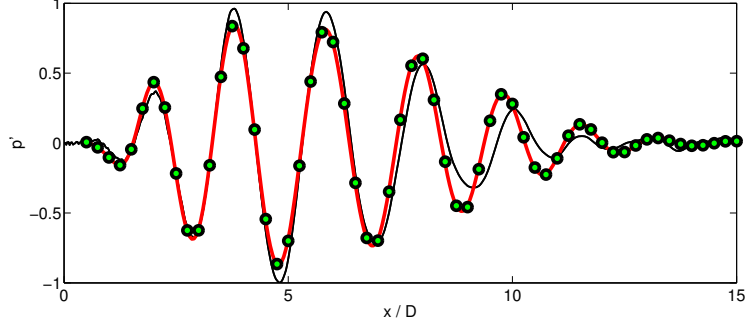


FIGURE 3. Wavepacket at  $St = 0.35$  along  $r/D = 0.5$ . Thin black line: first POD mode of the LES data; thick red line: first POD mode of the ensemble of PSE with different short-time-averaged mean flows; circles: PSE with long-time-averaged mean. The real part of the pressure eigenfunctions are plotted.

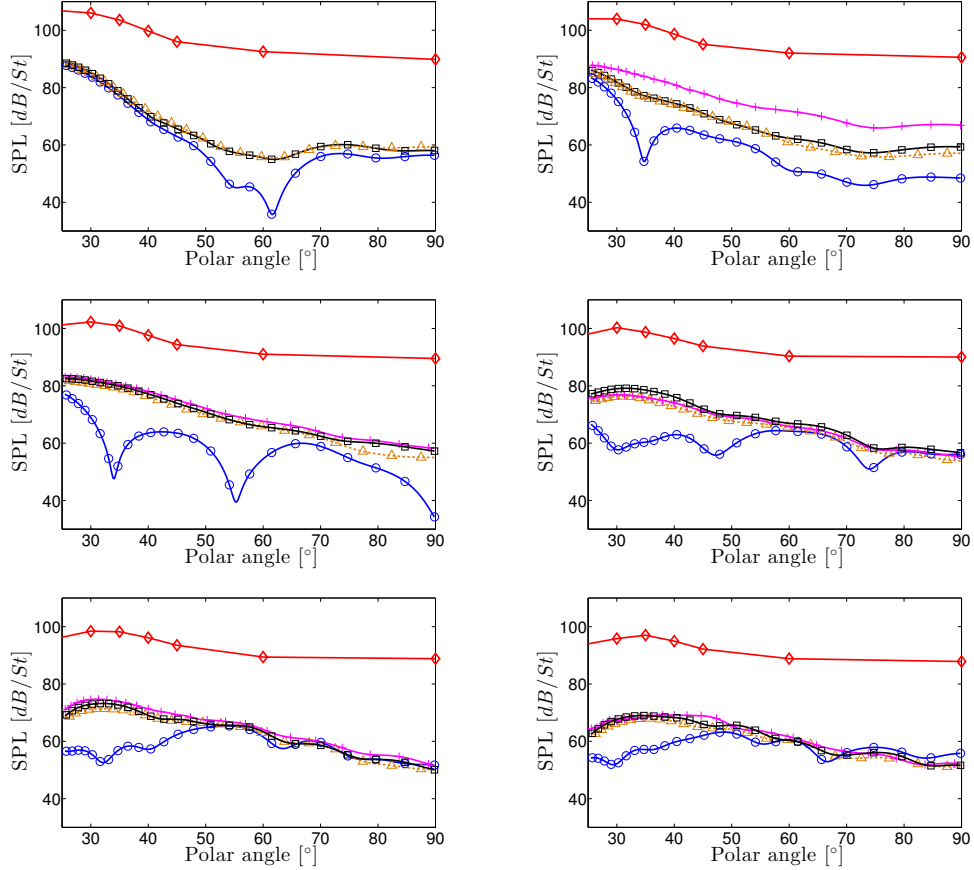


FIGURE 4. SPL, as a function of emission angle, for  $m = 0$  wavepacket. Solid line with diamonds: LES; solid line with circles: SLEE; solid line with squares: ULEE run for time  $tc_\infty/D = 400$  ( $c_\infty$  is the ambient sound speed); solid line with triangles: ULEE run for time  $tc_\infty/D = 1000$ ; solid line with crosses: ULEE forced with five frequencies ( $St = [0.35, 0.43, 0.52, 0.61, 0.69]$ ). (a)  $St = 0.26$ . (b)  $St = 0.35$ . (c)  $St = 0.43$ . (d)  $St = 0.52$ . (e)  $St = 0.61$ . (f)  $St = 0.69$ .

by such lobes, the directivity patterns being significantly improved. But the main conclusion to be drawn from Figure 4 is that while the acoustic efficiency of wavepackets is considerably boosted by the incorporation of jitter, amplifications of up to 20dB being observed (multiple-frequency forcing showing non-linear effects to produce additional amplification for  $St = 0.35$ ), this is not sufficient to explain the radiation efficiency of the wavepackets that exist in the LES and the experiment.

The PSE/OWE results for an ensemble of steady, short-time-averaged base flows, are similar to what is predicted by the ULEE. Their close agreement shows that the inclusion of an unsteady base flow, at least a slowly varying one, produces the same effect as an ensemble of different base flows. In Figure 3, the coherent near-field wavepacket deduced by applying POD to an ensemble of PSE with different short-time-averaged base flows is compared to that from the LES and to the PSE wavepacket associated with the long-time-averaged flow. In the figure, the short-time averages were made over a period corresponding to a Strouhal number of 0.08, but we also considered periods half and twice as long with very similar results<sup>†</sup>. The figure shows that the variations in the base flow did not give rise to any significant change in the near-field, averaged wavepacket, similar to what is observed above for ULEE.

In Figure 5, we go on to plot the coherence at  $St = 0.35$  between the point where the wavepacket at this frequency attains its maximum amplitude and points along the jet lip-line<sup>‡</sup>. Results are shown for the LES data as well as for the ensemble of PSE solutions for the short-time-averaged flow field. For the figure, the short-time averages were made over a period corresponding to a Strouhal number of 0.08, but we also considered periods half and twice as long with very similar results. Also included in the figure is the coherence reconstructed from a few POD modes of the LES fluctuations. While one would not, in general, expect a match between the simple linear models and the full coherence of the turbulence, the comparison of the models with low-order reconstructions reveals that variations in wavepackets due to the differences between the different short-time-averaged base flows is just one, and perhaps not the most important, source of intermittency of the wavepackets.

Thus while these results confirm hypotheses H1 and H2 and show that the incorporation of intermittency effects in the linear modeling of wavepackets is important, insofar as it leads to both significant sound amplification and more realistic directivity patterns in comparison to average wavepackets, it is clear that additional modeling elements are necessary if the kind of intermittency observed in the LES and experiment is to be reproduced. Two avenues have been identified using the LES database and are currently being investigated. The first is the introduction of realistic inlet forcing. All of the results presented here correspond to harmonic forcing with the LST Kelvin-Helmholtz eigenfunction. The second element, which is the object of a separate study (Nichols 2014), is built on the idea that turbulence throughout the jet may act as a volumetric ‘external’ forcing for linear wavepackets (such a scenario has been proposed by Landahl (1967) and

<sup>†</sup> The different PSE realizations were calibrated by equating their amplitude near the nozzle exit with the LES wavepacket deduced by projecting the fluctuations at the corresponding frequency (for the same short-time-average bin) onto the first POD mode of the entire dataset. This procedure is rationalized by the very close agreement between POD and PSE for the initial growth of the wavepacket.

<sup>‡</sup> For a discussion of the connection between the two-point coherence of wavepackets and their sound radiation, the reader should refer to Cavalieri & Agarwal (2014) and Baqui *et al.* (2014).

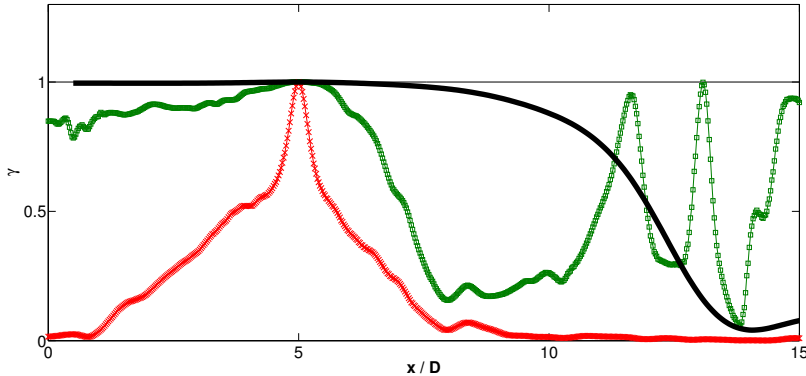


FIGURE 5. Coherence at  $St = 0.35$  between the point  $x/D = 5, r/D = 0.5$  and other points along  $r/D = 0.5$ . Red crosses: LES; green squares: 2-POD-mode reconstruction of the LES data; thick black line: ensemble of PSE with different short-time-averaged mean flows; thin black line: 1-POD-mode reconstruction of the LES data.

is more recently being explored by McKeon & Sharma (2010) in the context of boundary layers). Further work is required to clarify the respective importance of these phenomena.

#### 4. Concluding remarks

Wavepacket intermittency, which appears to be a key to understanding and modeling subsonic jet noise, has been considered by the combined use of high-fidelity numerical simulation data and simplified linear models. The phenomenon was incorporated in the models via the introduction of time-varying base flows, in both statistical and time-dependent frameworks. Jittering wavepackets with considerably enhanced acoustic efficiency were successfully generated. But the results show that the modeling framework requires further additions if the observed (LES and experimental) radiation levels are to be matched. Two such additions, identified during the summer program as important, are: (i) the use of realistic inflow forcing, as opposed to the harmonic Kelvin-Helmholtz-eigenmode forcing used here; and (ii), the incorporation of volumetric forcing by turbulence (Nichols 2014).

A second outcome of this study was the validation of a novel spatial marching technique, OWE, which alleviates several shortcomings of the PSE method and which can produce results equivalent to the full LEE at a fraction of the computational cost.

#### REFERENCES

- BAQUI, Y., AGARWAL, A. & CAVALIERI, A. V. G. 2014 A coherence-matched linear model for subsonic jet noise. In *20th AIAA/CEAS Aeroacoustics Conference*.
- BREAKY, D., JORDAN, P., CAVALIERI, A., LEON, O., ZHANG, M., LEHNASCH, G., COLONIUS, T. & RODRIGUEZ, D. 2013 Near-field wavepackets and the far-field sound of a subsonic jet. In *19th AIAA/CEAS Aeroacoustics Conference, Paper 2013-2083*.
- BRÈS, G. A., JORDAN, P., COLONIUS, T., LE RALLIC, M., JAUNET, V. & LELE, S. K. 2014 Large eddy simulation of a Mach 0.9 turbulent jet. *Proceedings of the Summer Program*, Center for Turbulence Research, Stanford University.

- CAVALIERI, A. V. G. & AGARWAL, A. 2014 Coherence decay and its impact on sound radiation by wavepackets. *J. Fluid Mech.* **748**, 399–415.
- CAVALIERI, A. V. G., JORDAN, P., AGARWAL, A. & GERVAIS, Y. 2011 Jittering wavepacket models for subsonic jet noise. *J. Sound Vib.* **330**, 4474–4492.
- CAVALIERI, A. V. G., RODRGUEZ, D., JORDAN, P., COLONIUS, T. & GERVAIS, Y. 2013 Wavepackets in the velocity field of turbulent jets. *J. Fluid Mech.* **730**, 559–592.
- GUDMUNDSSON, K. & COLONIUS, T. 2011 Instability wave models for the near-field fluctuations of turbulent jets. *J. Fluid Mech.* **689**, 97–128.
- HAGSTROM, T. & WARBURTON, T. 2004 A new auxiliary variable formulation of high-order local radiation boundary conditions: corner compatibility conditions and extensions to first-order systems. *Wave Motion* **39**, 890–901.
- HERBERT, T. 1997 Parabolized stability equations. *Ann. Rev. Fluid Mech.* **29**, 245–283.
- JORDAN, P. & COLONIUS, T. 2013 Wave packets and turbulent jet noise. *Ann. Rev. Fluid Mech.* **45**, 173–195.
- JUVÉ, D., SUNYACH, M. & COMTE-BELLOT, G. 1980 Intermittency of the noise emission in subsonic cold jets. *J. Sound Vib.* **71**, 319–332.
- KERHERVÉ, F., JORDAN, P., CAVALIERI, A. V. G., DELVILLE, J., BOGEY, C., JUVÉ, D. *et al.* 2012 Educting the source mechanism associated with downstream radiation in subsonic jets. *J. Fluid Mech.* **710**, 1–32.
- KOENIG, M., CAVALIERI, A. V. G., JORDAN, P., DELVILLE, J., GERVAIS, G. & PAPAMOSCHOU, D. 2012 Farfield filtering and source imaging of subsonic jet noise. *J. Sound Vib.* **18**, 4067–4068.
- LANDAHL, M. T. 1967 A wave-guide model for turbulent shear flow. *J. Fluid Mech.* **29**, 441–459.
- MCKEON, B. & SHARMA, A. 2010 A critical-layer framework for turbulent pipe flow. *J. Fluid Mech.* **658**, 336–382.
- NICHOLS, J. 2014 Input-output analysis of high-speed jet noise. *Proceedings of the Summer Program*, Center for Turbulence Research, Stanford University.
- SANDBERG, R. D. & SANDHAM, N. D. 2006 Nonreflecting zonal characteristic boundary condition for direct numerical simulation of aerodynamic sound. *AIAA Journal* **44**, 402–405.
- TOWNE, A. & COLONIUS, T. 2013 Improved parabolization of the Euler equations. In *19th AIAA/CEAS Aeroacoustics Conference, AIAA Paper 2013-2171*.
- TOWNE, A. & COLONIUS, T. 2014 Continued development of the one-way Euler equations: application to jets. In *20th AIAA/CEAS Aeroacoustics Conference, AIAA Paper 2014-2903*.
- ZHANG, M., JORDAN, P., LEHNASCH, G., CAVALIERI, A. & AGARWAL, A. 2014 Just enough jitter for jet noise? In *20th AIAA/CEAS Aeroacoustics Conference, AIAA Paper 2014-3061*.